

MA-112

ey4



NOZZLE TURBULENT BOUNDARY-LAYER MEASUREMENTS IN THE VKF 50-IN. HYPERSONIC TUNNELS

R. K. Matthews and L. L. Trimmer

ARO, Inc.

June 1969

This document is subject to special export controls and each transmittal to foreign governments or foreign nationals may be made only with prior approval of Arnold Engineering Development Center (AETS), Arnold Air Force Station, Tennessee 37389.

This document has been approved for public release its distribution is unlimited.

Per AF Letter
dtd 25 March 1976
Army W.O. Cole
Strif

VON KÁRMÁN GAS DYNAMICS FACILITY
ARNOLD ENGINEERING DEVELOPMENT CENTER
AIR FORCE SYSTEMS COMMAND
ARNOLD AIR FORCE STATION, TENNESSEE

NOTICES

When U. S. Government drawings specifications, or other data are used for any purpose other than a definitely related Government procurement operation, the Government thereby incurs no responsibility nor any obligation whatsoever, and the fact that the Government may have formulated, furnished, or in any way supplied the said drawings, specifications, or other data, is not to be regarded by implication or otherwise, or in any manner licensing the holder or any other person or corporation, or conveying any rights or permission to manufacture, use, or sell any patented invention that may in any way be related thereto.

Qualified users may obtain copies of this report from the Defense Documentation Center.

References to named commercial products in this report are not to be considered in any sense as an endorsement of the product by the United States Air Force or the Government.

NOZZLE TURBULENT BOUNDARY-LAYER MEASUREMENTS
IN THE VKF 50-IN. HYPERSONIC TUNNELS

R. K. Matthews and L. L. Trimmer
ARO, Inc.

This document is subject to special export controls and each transmittal to foreign governments or foreign nationals may be made only with prior approval of Arnold Engineering Development Center (AEDC), Arnold Air Force Station, Tennessee 37389.

This document has been approved for public release
its distribution is unlimited.

Per AF Letter
dt'd 25 March 1976
signed W.O. Cole, Strife

FOREWORD

The work reported herein was sponsored by the Arnold Engineering Development Center (AEDC), Air Force Systems Command (AFSC), Arnold Air Force Station, Tennessee, under Program Element 65401F, Program 876A, Project G266.

The results of research presented were obtained by ARO, Inc. (a subsidiary of Sverdrup & Parcel and Associates, Inc.), contract operator of AEDC, AFSC, under Contract F40600-69-C-0001. The work was done under ARO Project Numbers VT3116 and VT2914, during the period from March to July, 1965, and the manuscript was submitted for publication on April 24, 1969.

Information in this report is embargoed under the Department of State International Traffic in Arms Regulations. This report may be released to foreign governments by departments or agencies of the U. S. Government subject to approval of the Arnold Engineering Development Center (AETS), or higher authority, within the Department of the Air Force. Private individuals or firms require a Department of State export license.

This technical report has been reviewed and is approved.

Eugene C. Fletcher
Lt Colonel, USAF
AF Representative, VKF
Directorate of Test

Roy R. Croy, Jr.
Colonel, USAF
Director of Test

ABSTRACT

Pitot pressure and total temperature measurements in the tunnel wall boundary layers in the von Karman Gas Dynamics Facility 50-in. -diam hypersonic wind tunnels are presented. The measurements were obtained in the wind tunnel test sections at nominal free-stream Mach numbers of 6, 8, and 10 at free-stream unit Reynolds numbers from 0.32×10^6 to 3.91×10^6 per foot. The boundary layers were fully turbulent (velocity profile index 6 to 10), and the total thickness ranged from 4 to 11 in. Velocity and mass flow profiles were computed and used to calculate boundary-layer displacement and momentum thicknesses. The experimentally determined ratio of displacement thickness to momentum thickness was essentially independent of Mach number and Reynolds number over the ranges investigated.

This document is subject to special export controls and each transmittal to foreign governments or foreign nationals may be made only with prior approval of Arnold Engineering Development Center (AEDC), Arnold Air Force Station, Tennessee 37389.

This document has been approved for public release
its distribution is unlimited

Per AF Letter dtd 25 March 1976
Signed by W.O. Cole, STNFO

CONTENTS

	<u>Page</u>
ABSTRACT	iii
NOMENCLATURE	vi
I. INTRODUCTION	1
II. APPARATUS	
2.1 Wind Tunnels	1
2.2 Test Equipment	2
III. PROCEDURE	3
IV. RESULTS AND DISCUSSION	5
V. CONCLUSIONS	6
REFERENCES	7

APPENDIXES

I. ILLUSTRATIONS

Figure

1. VKF Wind Tunnels B and C	
a. Tunnel Assembly	11
b. Tunnel Test Section	11
2. Wind Tunnel Geometry	12
3. Boundary-Layer Probe Details	13
4. Nondimensional Velocity Profiles	
a. $M_e = 6$	14
b. $M_e = 8$	14
c. $M_e = 10$	15
5. Velocity Profile Index (n) Variation with Reynolds Number	16
6. Correlation of Total Temperature Measurements	16
7. Effect of Reynolds Number on Boundary-Layer Thicknesses	17
8. Summary of Boundary-Layer Measurements	18
II. DATA AND TEST CONDITIONS	19

NOMENCLATURE

H	δ^*/θ , form factor
M	Mach number
n	Velocity profile index, $(u/u_e) = (y/\delta)^{1/n}$
p	Pressure, psia
Pr	Prandtl number
R	Gas constant, $1716.3 \frac{\text{ft}^2}{\text{sec}^2 \cdot \text{°R}}$
Re	Unit Reynolds number based on boundary-layer edge conditions, ft^{-1}
Re _x	Reynolds number based on boundary-layer edge conditions and distance from throat to survey station (e. g., x_{2-4} in Fig. 2)
r	Radius of tunnel, in.
T	Temperature, °R
u	Velocity, ft/sec
x	Tunnel axial distances (see Fig. 2), in.
y	Distance from tunnel wall, in.
γ	Ratio of specific heats
δ	Boundary-layer thickness, in.
δ^*	Boundary-layer displacement thickness, in.
θ	Boundary-layer momentum thickness, in.
ρ	Density, slugs/ft ³

SUBSCRIPTS

e	Boundary-layer edge conditions
o	Stilling chamber conditions
p	Probe conditions
w	Nozzle wall conditions

SECTION I INTRODUCTION

The designers of contoured wind tunnel nozzles must be able to make accurate predictions of the nozzle boundary-layer growth. The method generally used in the design of supersonic and hypersonic wind tunnel nozzles is to add the estimated boundary-layer displacement thickness to the inviscid nozzle coordinates. Thus, the mass flow defect caused by the viscous boundary-layer flow is accounted for. Nozzle coordinates for inviscid flow are generally calculated by the method of characteristics (Ref. 1). Most hypersonic wind tunnel nozzle boundary layers are turbulent, and calculation of the displacement thickness requires semi-empirical methods (Refs. 2 and 3). Numerous studies of boundary layers in supersonic flow have been reported (Refs. 4 through 7); however, hypersonic flow boundary-layer studies (Refs. 8, 9, and 10) are not as numerous.

The large continuous hypersonic wind tunnels at the von Kármán Gas Dynamics Facility (VKF), AEDC, produce relatively thick (from 4 to 11 in.) turbulent boundary layers that are ideal for experimental study. Pitot pressure and total temperature surveys of the test section boundary layers were made in the 50-in. -diam Gas Dynamic Wind Tunnels, Hypersonic (B) and (C). These surveys were obtained for nominal test section Mach numbers of 6, 8, and 10 and free-stream unit Reynolds numbers ranging from 0.32×10^6 to $3.91 \times 10^6 \text{ ft}^{-1}$.

SECTION II APPARATUS

2.1 WIND TUNNELS

Tunnels B and C (Fig. 1, Appendix I) are continuous, closed-circuit, variable density wind tunnels with axisymmetric, water-cooled contoured nozzles and 50-in. -diam test sections. Interchangeable throat sections permit operation of Tunnel B at nominal Mach numbers of 6 and 8 and Tunnel C at nominal Mach numbers of 10 and 12. Basic tunnel dimensions relevant to the nozzle contours are presented in Fig. 2.

The tests were conducted over the following tunnel stilling chamber pressure ranges:

<u>Tunnel</u>	<u>Mach Number</u>	<u>p₀ Range, psia</u>
B	6	50 to 300
B	8	100 to 800
C	10	200 to 1,800

Stilling chamber temperatures up to 1360°R were provided in Tunnel B by a natural-gas-fired combustion heater. Tunnel C stilling chamber temperatures up to 1970°R were provided by an electric resistance heater in conjunction with the gas-fired heater. These stilling chamber temperatures are sufficient to prevent liquefaction of the air as it is expanded to test section conditions. Additional information on the design and operation of Tunnels B and C is available in Ref. 11.

2.2 TEST EQUIPMENT

The boundary-layer probe location in the wind tunnels is shown in Fig. 2, and the probe geometry is shown in Fig. 3. The combination pitot pressure and total temperature probe was traversed in a direction normal to the tunnel centerline. The slope of the tunnel wall relative to the tunnel centerline was less than 0.5 deg at the survey station, and the associated error in probe height was neglected. Also, as noted in Fig. 3, the total temperature probe was located in the tunnel vertical plane of symmetry, whereas the pitot probe was located 0.8 in. to the side. The error in pitot probe location produced by assuming equal y values for both measurements was less than 0.02 in. and was neglected because the estimated probe positioning precision is ±0.05 in.

Probe pressure was measured with a 15-psid transducer which, from repeat calibrations, is estimated to have been precise within ±0.003 psia or 0.5 percent, whichever was greater. A Chromel®-Alumel® thermocouple was used in the double-shielded, vented, total temperature probe. Calibrations of typical thermocouples have shown the indicated temperatures to be accurate within ±2°R or 0.5 percent, whichever is greater. Operation of the probe, however, indicated total temperatures as much as 10 percent lower than T₀ for probe readings taken in the free-stream at the lowest tunnel Reynolds numbers. These errors are attributed primarily to probe internal viscous losses and secondarily to conduction and radiation losses (Ref. 12).

SECTION III PROCEDURE

Boundary-layer measurements are normally limited to pitot pressure and total temperature surveys. Several assumptions are required to reduce these measurements to the boundary-layer parameters δ^* and θ . Boundary-layer pitot pressures can be converted to Mach numbers by assuming a knowledge of the local static pressure and application of the Rayleigh pitot formula. The free-stream static pressure (calculated from the edge Mach number and stilling chamber pressure) is generally assumed constant across the boundary layer and was the procedure used herein. This assumption should be viewed in light of the fact that some static pressure gradient through the boundary layer (up to 10 percent) is expected because the nozzle flow is not completely expanded (that is, completely parallel) at the boundary-layer survey station. Unfortunately, measured wall static pressures were inconclusive.

Boundary-layer edge (free-stream) conditions in Tunnel B were calculated assuming a perfect gas isentropic expansion from the stilling chamber. Because of higher stagnation pressures and temperatures, the Tunnel C boundary-layer edge conditions were calculated assuming a real gas isentropic expansion using the Beattie-Bridgeman equation of state and procedures described in Ref. 13.

It is pointed out in Ref. 8 that the conventional method of defining δ (i. e., y where $u/u_e = 0.99$) is ill suited for hypersonic boundary layers because the velocity is greater than $0.99 u_e$ over a sizable portion of the boundary layer. That is, for $0.99 u_e$, the pitot pressure ranges from 0.96 to 0.95 pp_e for $M_e = 6$ to 10, respectively. In addition, pitot pressure profiles were subject to inviscid flow nonuniformities as well as viscous effects and, therefore, may bias the determination of δ . For the present work, the total temperature profiles were used to define δ (i. e., a loss in total temperature was attributed solely to viscous effects). The boundary-layer thickness was chosen as the y value where $T_p/T_{pe} = 0.995$. In the hypersonic limit (Ref. 10), when the Mach number becomes infinite in the outer portion of the boundary layer, the total temperature can be related to the velocity by neglecting the static temperature term in the energy equation. Nondimensionalizing by boundary-layer edge conditions gives

$$\frac{T_p}{T_{pe}} = \left(\frac{u}{u_e}\right)^2 \text{ for } y \rightarrow \delta \quad (1)$$

The selection of δ at $T_p/T_{pe} = 0.995$ then corresponds to a velocity ratio (from Eq. (1)) of about 0.998.

The basic total temperature and pitot pressure measurements are presented (in plotted form) in Figs. II-1 and II-2, respectively (Appendix II). The values selected for δ are indicated on the total temperature profiles (Fig. II-1) and are also shown for comparison on the pitot pressure profiles (Fig. II-2). Note, as discussed in Section 2.2, that for some test conditions the total temperature probe did not agree with the stilling chamber temperature ($T_{pe}/T_o \neq 1$) when in the free stream. In these cases, the value of T_{pe} was adjusted to agree with T_o , and all boundary-layer temperature measurements were similarly adjusted (multiplied) by the experimental ratio, T_o/T_{pe} .

Assuming a thermally perfect gas (i. e. , $p = \rho RT$), the boundary-layer velocities were calculated by the equation

$$u = M\sqrt{\gamma RT} \tag{2}$$

where: M was calculated as previously described

$$T = \frac{T_p}{\left(1 + \frac{\gamma - 1}{2} M^2\right)} \tag{3}$$

and $\gamma = 1.4$

Combining Eq. (2) with the perfect gas equation of state yields the local mass flow

$$\rho u = \left(\frac{p}{RT}\right) \left(M\sqrt{\gamma RT}\right) \tag{4}$$

where p is assumed equal to p_e (i. e. , $(dp/dy) = 0$).

The displacement thickness for a two-dimensional boundary layer is defined by

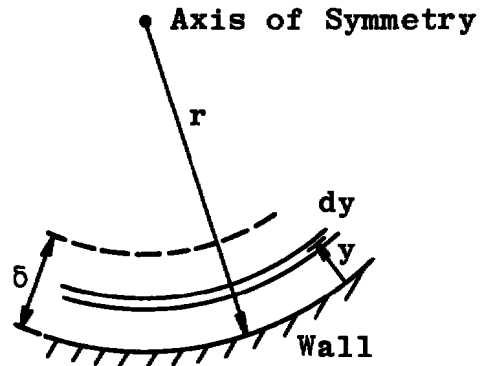
$$\delta^* = \int_0^\delta \left(1 - \frac{\rho u}{\rho_e u_e}\right) dy \tag{5}$$

The corresponding equation for an axisymmetric boundary layer can be shown, by considering the geometry of the sketch below, to be

$$\pi \left[r^2 - (r - \delta^*)^2 \right] = \int_{\pi r^2}^{\pi(r-\delta)^2} \left(1 - \frac{\rho u}{\rho_e u_e}\right) dA \tag{6}$$

where

$$dA = 2\pi (r - y) dy$$



Substituting for dA and reducing Eq. (6) gives

$$\delta^* \left(1 - \frac{\delta^*}{2r}\right) = \int_0^\delta \left(1 - \frac{\rho u}{\rho_e u_e}\right) \left(1 - \frac{y}{r}\right) dy \quad (7)$$

Similarly, the axisymmetric equation for the boundary-layer momentum thickness is

$$\theta \left(1 - \frac{\theta}{2r}\right) = \int_0^\delta \left(\frac{\rho u}{\rho_e u_e}\right) \left(1 - \frac{u}{u_e}\right) \left(1 - \frac{y}{r}\right) dy \quad (8)$$

The values of δ^* and θ for the present tests were obtained after a numerical integration of the right-hand sides of Eqs. (7) and (8). A summary of these boundary-layer characteristics, as well as the test conditions, is given in Table II-1, Appendix II.

SECTION IV RESULTS AND DISCUSSION

Nondimensional velocity profiles for Mach numbers 6, 8, and 10 at Reynolds numbers representative of the range covered are presented in Fig. 4. The profiles exhibit the typical turbulent "full" shape, and an exponential profile with $n = 9$ is shown for comparison purposes. The velocity profile index (n) for each survey was evaluated from the slope of u/u_e versus y/δ plotted on log-log paper. These experimentally

determined values of n are shown in Fig. 5. A free-stream Reynolds number, based on the nozzle length to the survey point, was chosen for the abscissa, and it is observed that essentially no Mach number trend exists. A definite trend of increasing n with Reynolds number is observed, and considering the precision of n (about ± 0.5), the correlation is quite good for the limited range of the present study.

Total temperature measurements selected from data at each Mach number (Fig. 6) are compared with predictions relating the total temperature to the velocity. The departure of turbulent boundary-layer total temperature profiles from the Crocco relation ($Pr = 1$) is discussed in Refs. 3 and 10. The present data were found to lie between the $(u/u_e)^2$ curve and the "hypersonic limit" which was discussed in Section III. Of course, these expressions cannot be expected to be valid near the wall where heat-transfer effects are strong (Ref. 3).

The variations of the boundary-layer thicknesses (δ , δ^* , and θ) with free-stream unit Reynolds number are presented in Fig. 7. Comparison of the δ^* values with the predictions of Sivells (Ref. 3) are generally within 10 percent.

A summary of the boundary-layer measurements in terms of H is shown in Fig. 8. It is significant to note that no trend with either Mach number or free-stream unit Reynolds number was found. This result was predicted by Sivells (Ref. 3); however, the predicted magnitude of H is approximately 30 percent high.

SECTION V CONCLUSIONS

Pitot pressure and total temperature distributions were measured in the tunnel wall boundary layers in the VKF 50-in.-diam hypersonic wind tunnels at free-stream Mach numbers 6, 8, and 10 and free-stream unit Reynolds numbers from 0.32×10^6 to 3.91×10^6 per foot. Within the limits of these test conditions, the results were as follows:

1. The boundary layers were fully turbulent. The velocity profile index (n) varied from 6 to 10 and was found to be dependent on free-stream Reynolds number, but essentially independent of free-stream Mach number.
2. The ratio of boundary-layer displacement thickness to momentum thickness (H or form factor) was essentially independent of free-stream Mach number and free-stream Reynolds number.

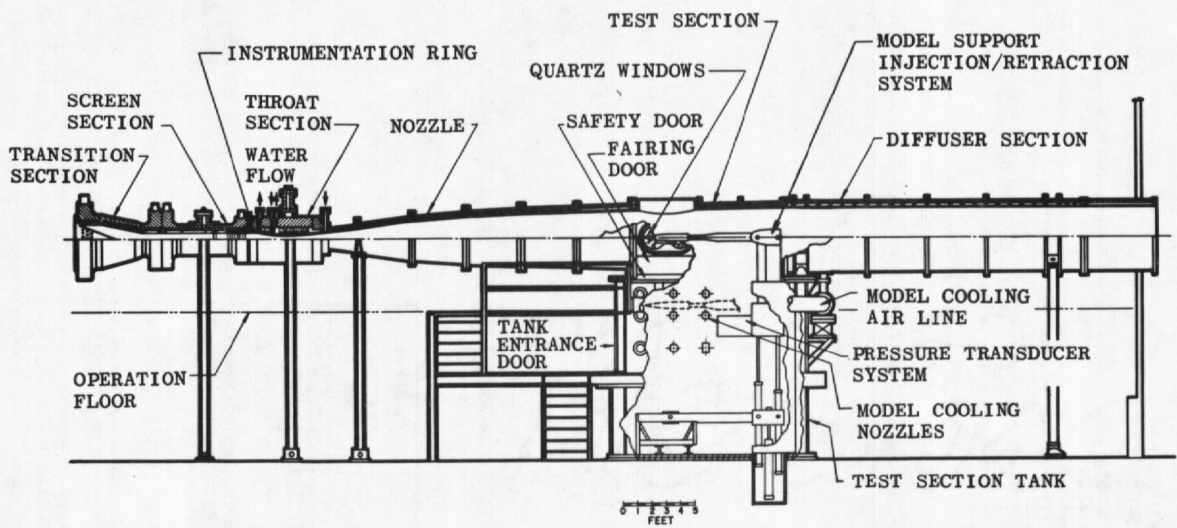
REFERENCES

1. Moger, W. C. and Ramsay, D. B. "Supersonic Axisymmetric Nozzle Design by Mass Flow Techniques Utilizing a Digital Computer." AEDC-TDR-64-110 (AD601589), June 1964.
2. Sivells, James C. and Payne, Robert G. "A Method of Calculating Turbulent-Boundary-Layer Growth at Hypersonic Mach Numbers." AEDC-TR-59-3 (AD208774), February 1959.
3. Sivells, James C. "Aerodynamic Design of Axisymmetric Hypersonic Wind Tunnel Nozzles." AIAA 4th Aerodynamics Testing Conference, Paper No. 69-337, Cincinnati, Ohio, April 28, 1969.
4. Jones, Jerry. "An Investigation of the Boundary-Layer Characteristics in the Test Section of a 40- by 40-Inch Supersonic Tunnel." AEDC-TN-60-189 (AD245362), October 1960.
5. Bell, D. R. "Boundary-Layer Characteristics at Mach Numbers 2 through 5 in the Test Section of the 12-Inch Supersonic Tunnel (D)." AEDC-TDR-63-192 (AD418711), September 1963.
6. Coles, Donald. "Measurements in the Boundary Layer on a Smooth Flat Plate in Supersonic Flow III. Measurements in a Flat-Plate Boundary Layer at the Jet Propulsion Laboratory." JPL Report No. 20-71, June 1, 1953.
7. Ruptash, J. "Boundary Layer Measurements in the UTIA 5- by 7-Inch Supersonic Wind Tunnel." UTIA Report No. 16, May 1952.
8. Scaggs, Norman E. "Boundary Layer Profile Measurements in Hypersonic Nozzles." ARL 66-0141, July 1966.
9. Perry, J. H. and East, R. A. "Experimental Measurements of Cold Wall Turbulent Hypersonic Boundary Layers." AGARD CP No. 30, May 1968.
10. Softley, Eric J. and Sullivan, Robert J. "Theory and Experiment for the Structure of Some Hypersonic Boundary Layers." AGARD CP No. 30, May 1968.
11. Sivells, James C. "Aerodynamic Design and Calibration of the VKF 50-Inch Hypersonic Wind Tunnels." AEDC-TDR-62-230 (AD299774), March 1963.
12. Bontrager, Paul J. "Development of Thermocouple-Type Total Temperature Probes in the Hypersonic Flow Regime." AEDC-TR-69-25 (AD681489), January 1969.

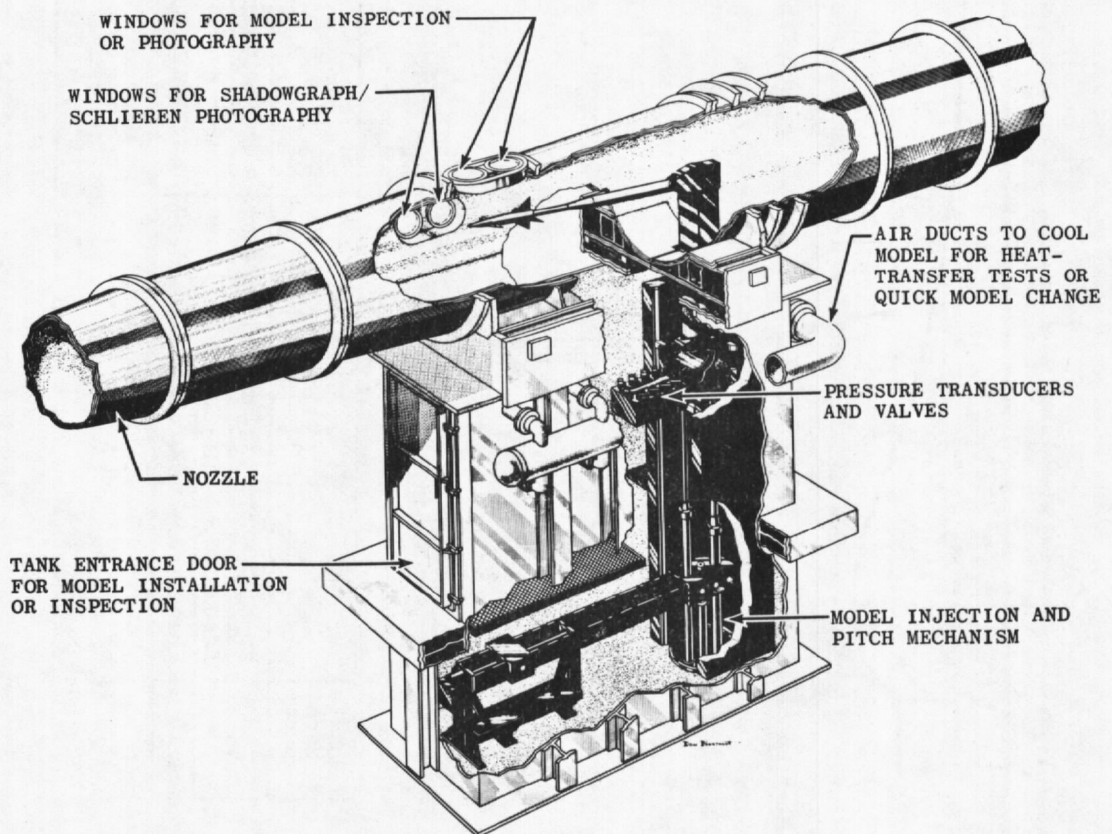
13. Randall, R. E. "Thermodynamic Properties of Air: Tables and Graphs Derived from the Beattie-Bridgeman Equation of State Assuming Variable Specific Heats." AEDC-TR-57-8 (AD135331), August 1957.

APPENDIXES

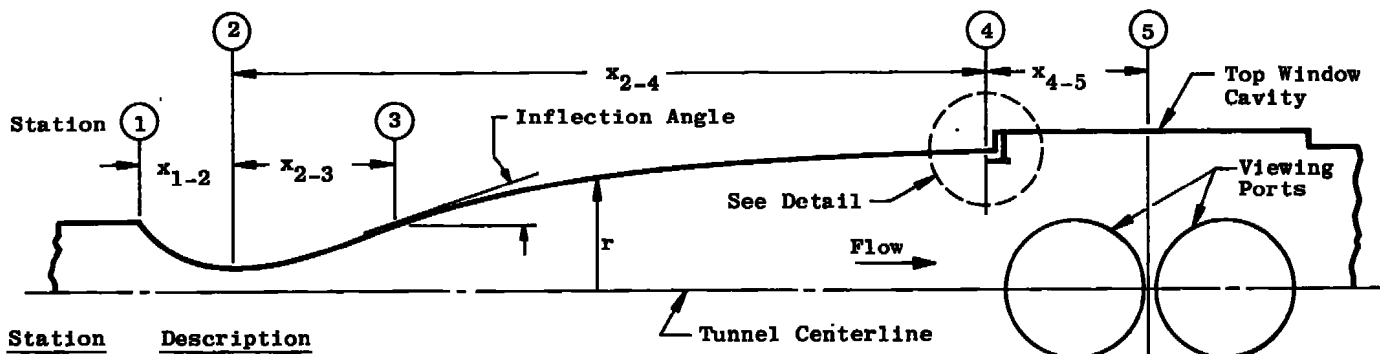
- I. ILLUSTRATIONS**
- II. DATA AND TEST CONDITIONS**



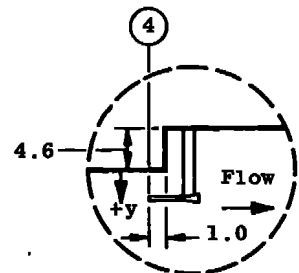
a. Tunnel Assembly



b. Tunnel Test Section
Fig. 1 VKF Wind Tunnels B and C



Station	Description
1	Begin Subsonic Contour
2	Throat
3	Inflection Point
4	Survey Station
5	Center of Test Section



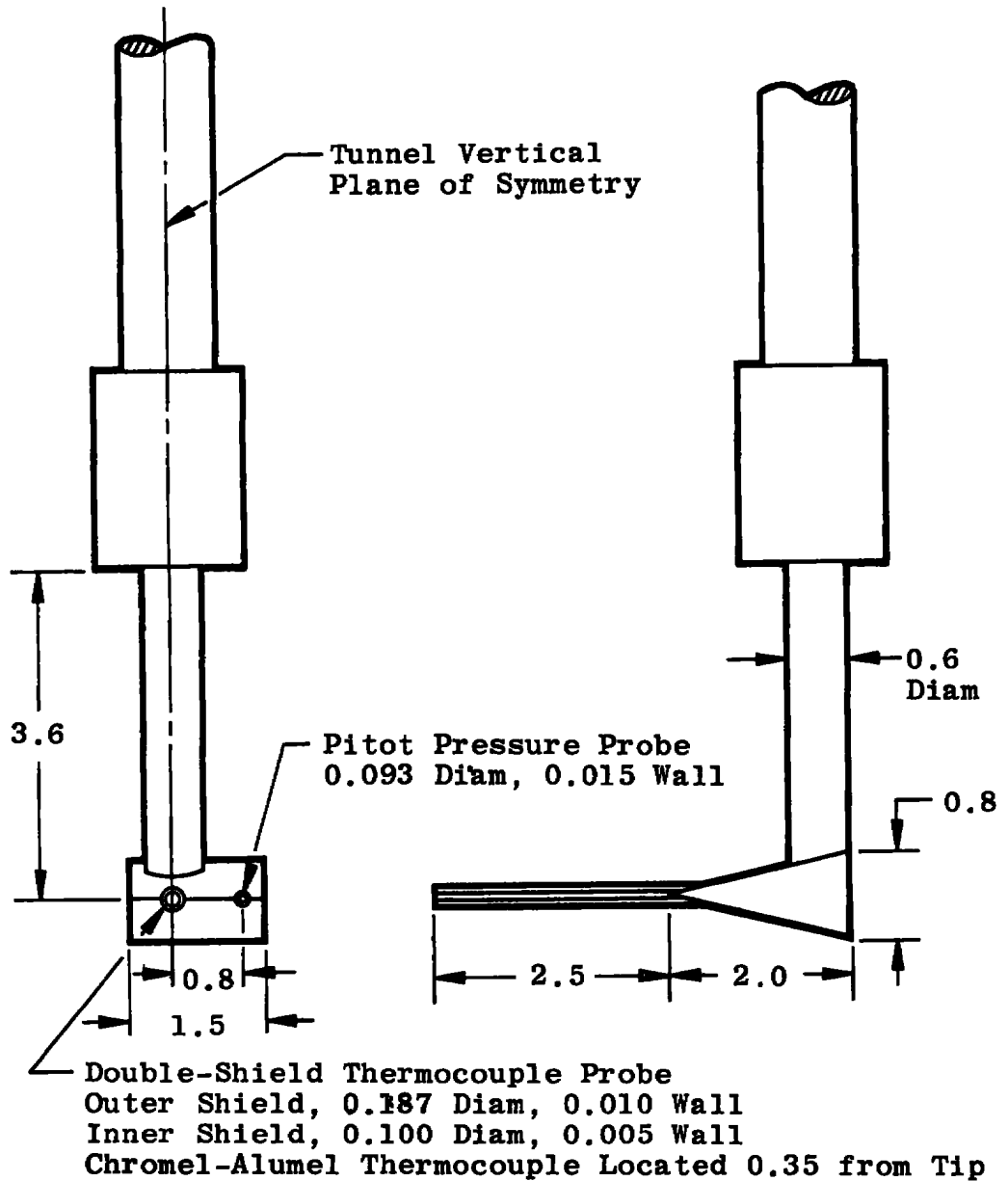
Probe Location Detail

x_3 x_4
50.27 273.85

Nozzle Mach Number	x_{1-2}	x_{2-3}	x_{2-4}	x_{4-5}	r_1	r_2	r_3	r_4	r_5	Inflection Angle, deg
6	31.92	18.37	242.08	21.50	6.00	3.171	6.33	24.34	24.64	12.52
8	24.66	25.63	249.19	21.50	6.00	1.584	6.33	24.34	24.64	12.52
10	20.57	33.43	301.93	21.50	6.00	0.873	5.71	24.34	24.64	9.06

All Dimensions in Inches
Sketches not to Scale

Fig. 2 Wind Tunnel Geometry



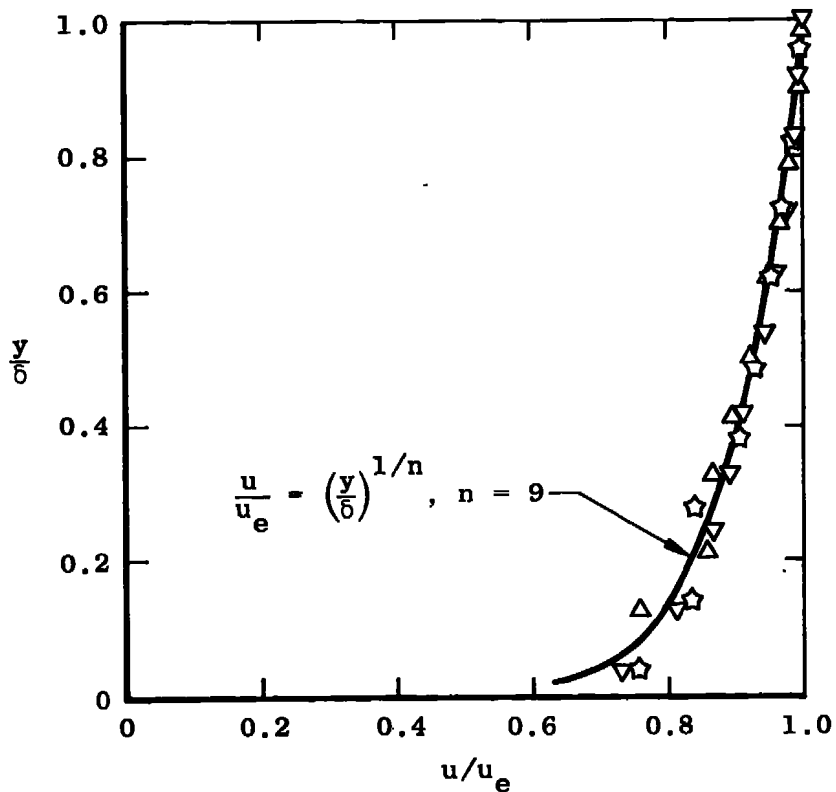
All Dimensions in Inches

Fig. 3 Boundary-Layer Probe Details

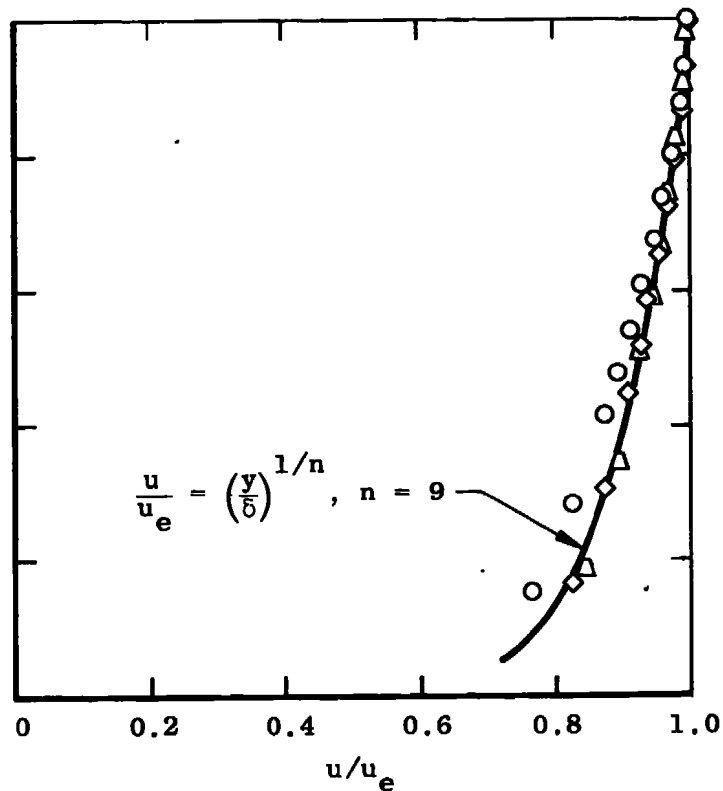
Sym	M_e	Re/ft $\times 10^{-6}$	δ , in.	u_e , ft/sec
Δ	5.93	1.04	5.25	2901
∇	5.91	2.04	5.10	2920
\star	5.95	3.91	4.40	2951

Sym	M_e	Re/ft $\times 10^{-6}$	δ , in.	u_e , ft/sec
\circ	7.90	0.44	7.73	3871
\diamond	7.96	1.73	7.15	3895
Δ	8.04	3.44	6.30	3860

14



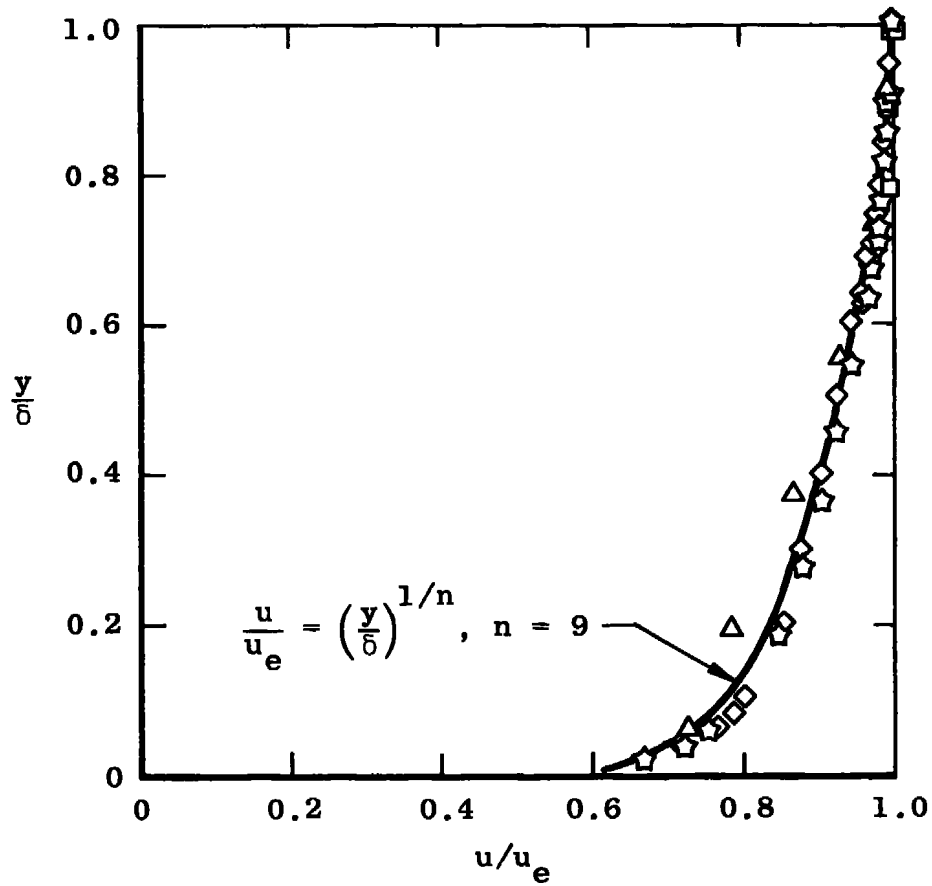
a. $M_e = 6$



b. $M_e = 8$

Fig. 4 Nondimensional Velocity Profiles

Sym	M_e	$Re/ft \times 10^{-6}$	δ , in.	u_e , ft/sec
Δ	9.86	0.32	11.1	4450
\star	10.10	1.14	11.0	4715
\diamond	10.18	2.03	9.9	4882



c. $M_e = 10$
 Fig. 4 Concluded

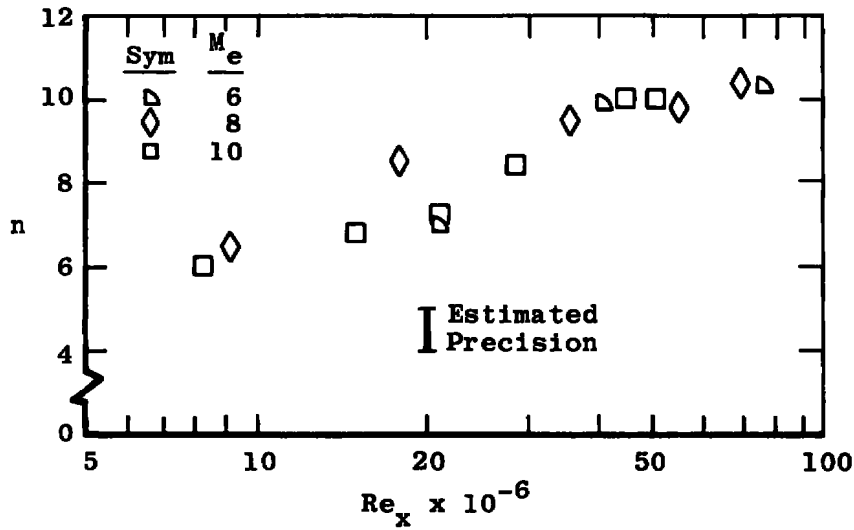


Fig. 5 Velocity Profile Index (n) Variation with Reynolds Number

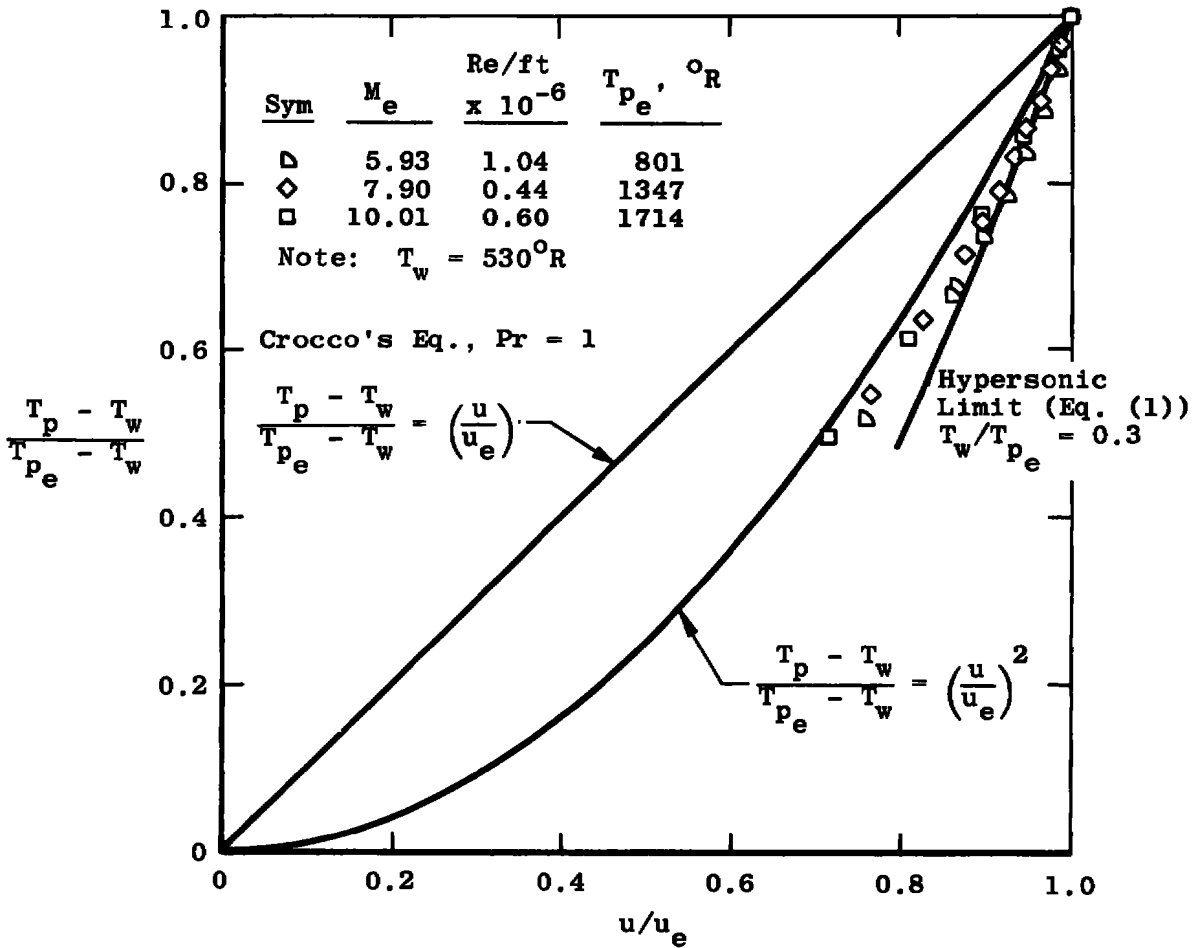


Fig. 6 Correlation of Total Temperature Measurements

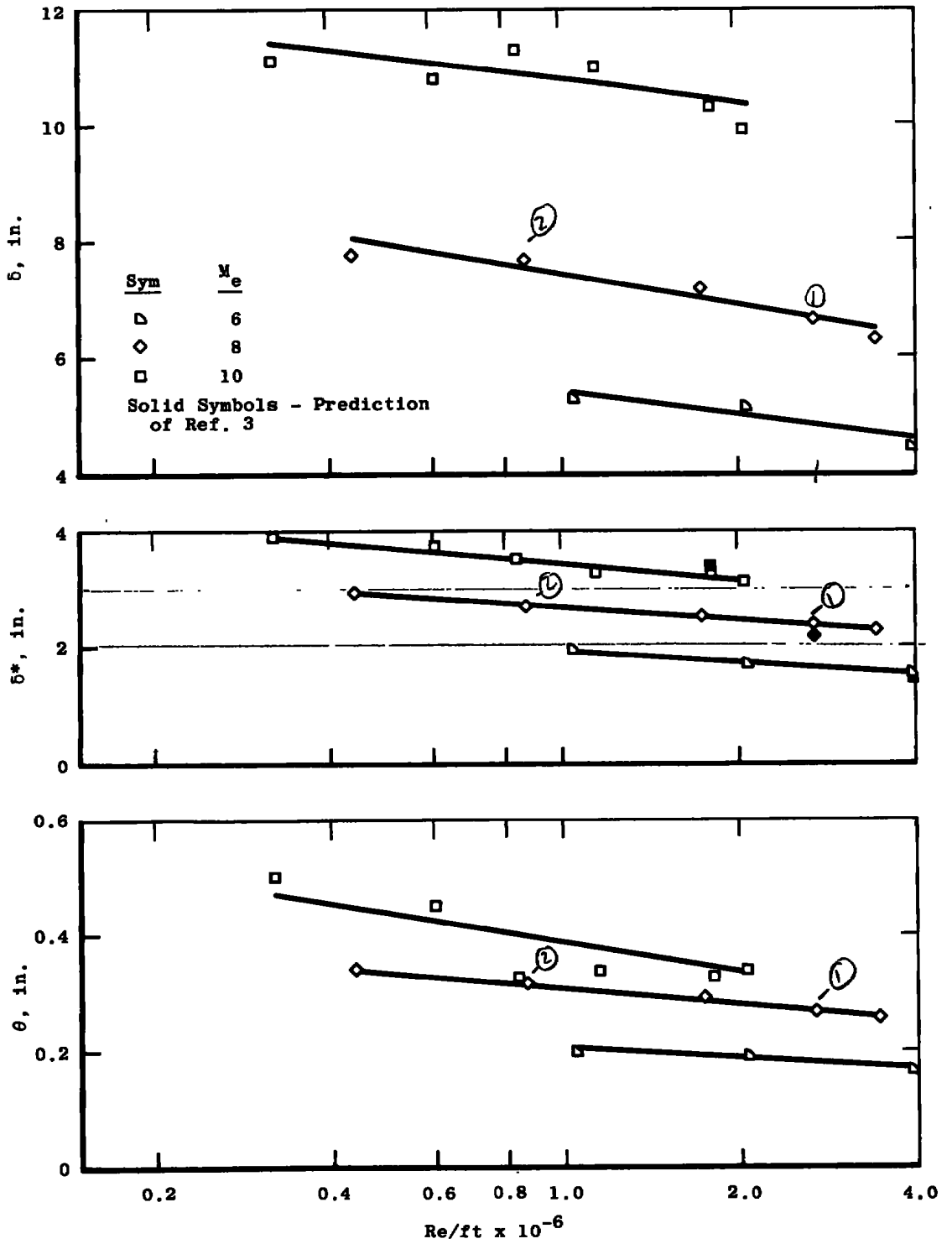


Fig. 7 Effect of Reynolds Number on Boundary-Layer Thicknesses

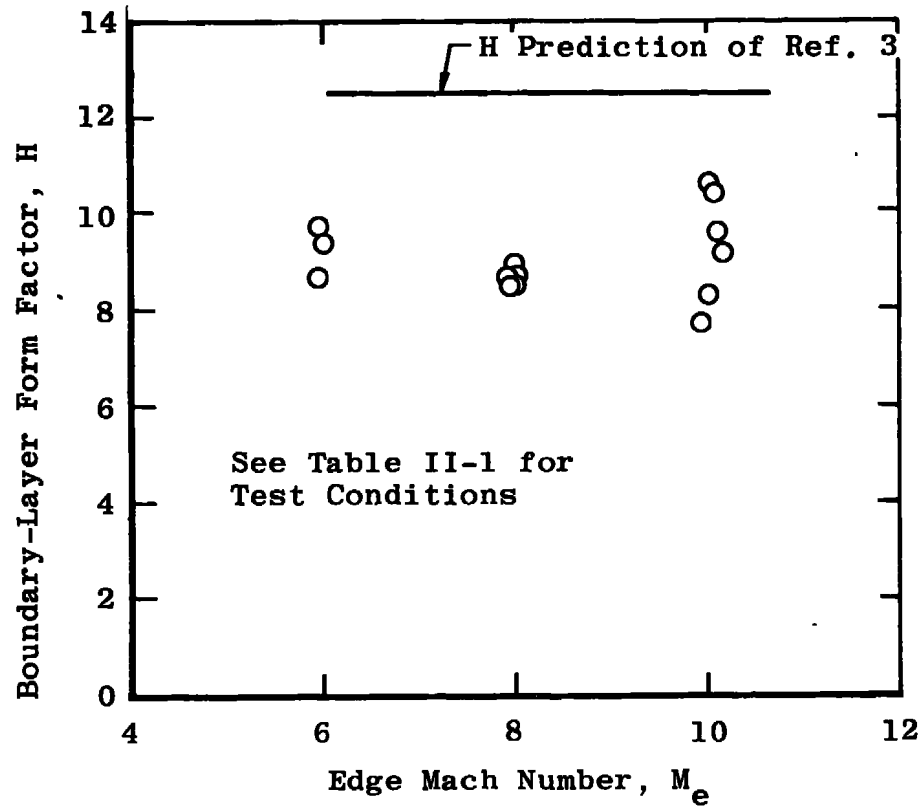


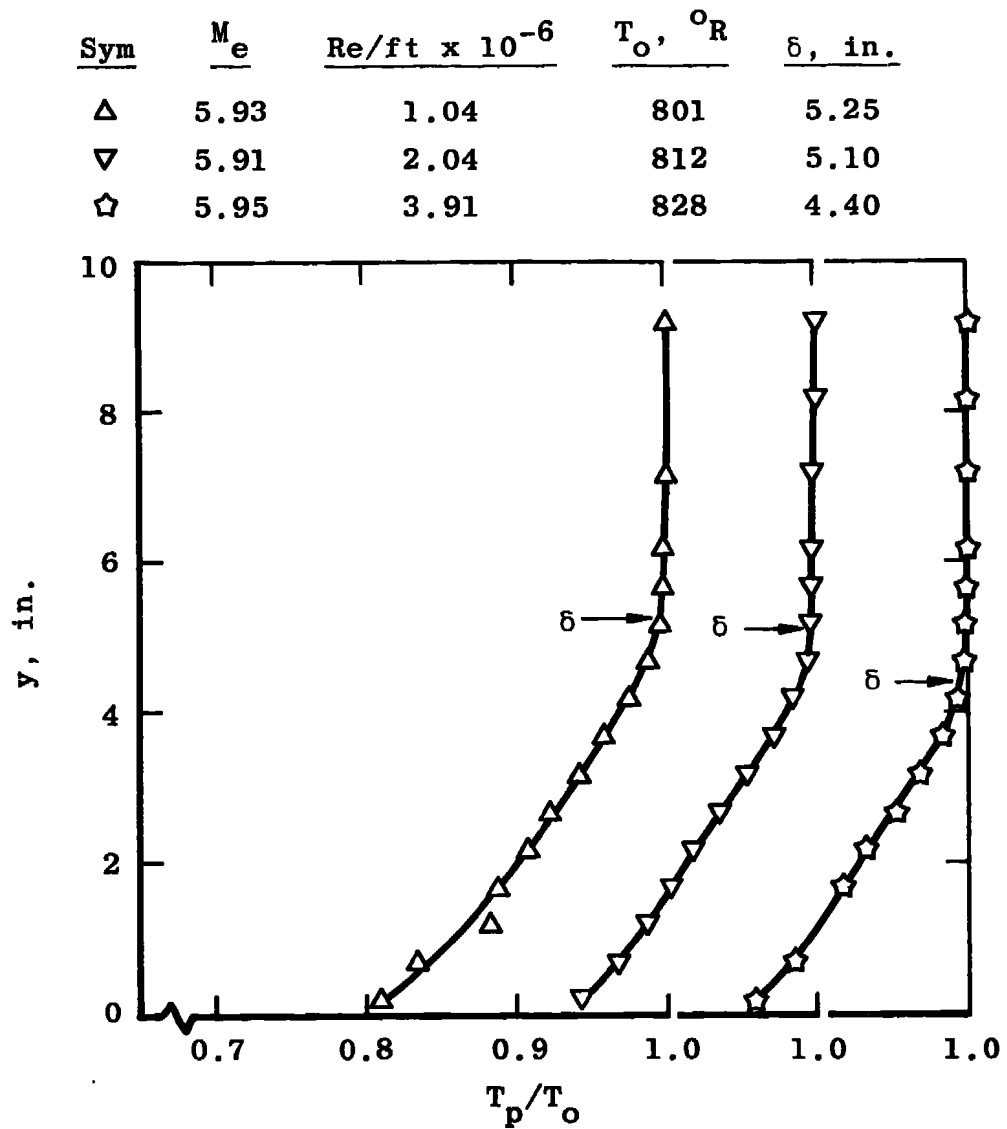
Fig. 8 Summary of Boundary-Layer Measurements

**APPENDIX II
DATA AND TEST CONDITIONS**

**TABLE II-1
SUMMARY OF TEST CONDITIONS AND BOUNDARY-LAYER CHARACTERISTICS**

M_e	$Re/ft \times 10^{-6}$	$x_{2-4}, in.$	$P_0, psia$	$T_0, ^\circ R$	$P_e, psia$	$T_e, ^\circ R$	$u_e, ft/sec$	$\rho_e \times 10^5, slugs/ft^3$	$\delta, in.$	$\delta^*, in.$	$\theta, in.$	H
5.93	1.04	242.08	50.2	801	0.034	99.8	2901	2.88	5.25	1.94	0.199	9.75
5.91	2.04	242.08	99.6	812	0.069	102	2920	5.72	5.10	1.62	0.187	8.65
5.95	3.91	242.08	200	828	0.134	103	2951	10.9	4.40	1.51	0.161	9.39
7.90	0.44	249.34	97.8	1347	0.011	99.8	3871	0.909	7.73	2.94	0.340	8.65
7.95	0.86	249.34	198	1359	0.021	99.5	3888	1.77	7.65	2.66	0.313	8.49
7.96	1.73	249.34	400	1362	0.042	99.6	3895	3.57	7.15	2.50	0.291	8.59
8.02	2.69	249.34	605	1321	0.061	95.4	3836	5.38	6.62	2.37	0.265	8.94
8.04	3.44	249.34	794	1337	0.079	96.0	3860	6.89	6.30	2.25	0.258	8.71
9.86	0.32	301.93	199	1672	0.005	84.7	4450	0.491	11.1	3.89	0.502	7.74
10.01	0.60	301.93	406	1714	0.009	84.7	4512	0.911	10.8	3.72	0.449	8.29
10.06	0.83	301.93	605	1775	0.013	87.2	4601	1.27	11.3	3.47	0.326	10.64
10.10	1.14	301.93	900	1854	0.019	90.7	4715	1.14	11.0	3.23	0.336	9.60
10.10	1.80	301.93	1500	1919	0.032	94.4	4810	2.85	10.3	3.25	0.313	10.30
10.18	2.03	301.93	1800	1969	0.037	95.9	4882	3.21	9.9	3.11	0.339	9.18

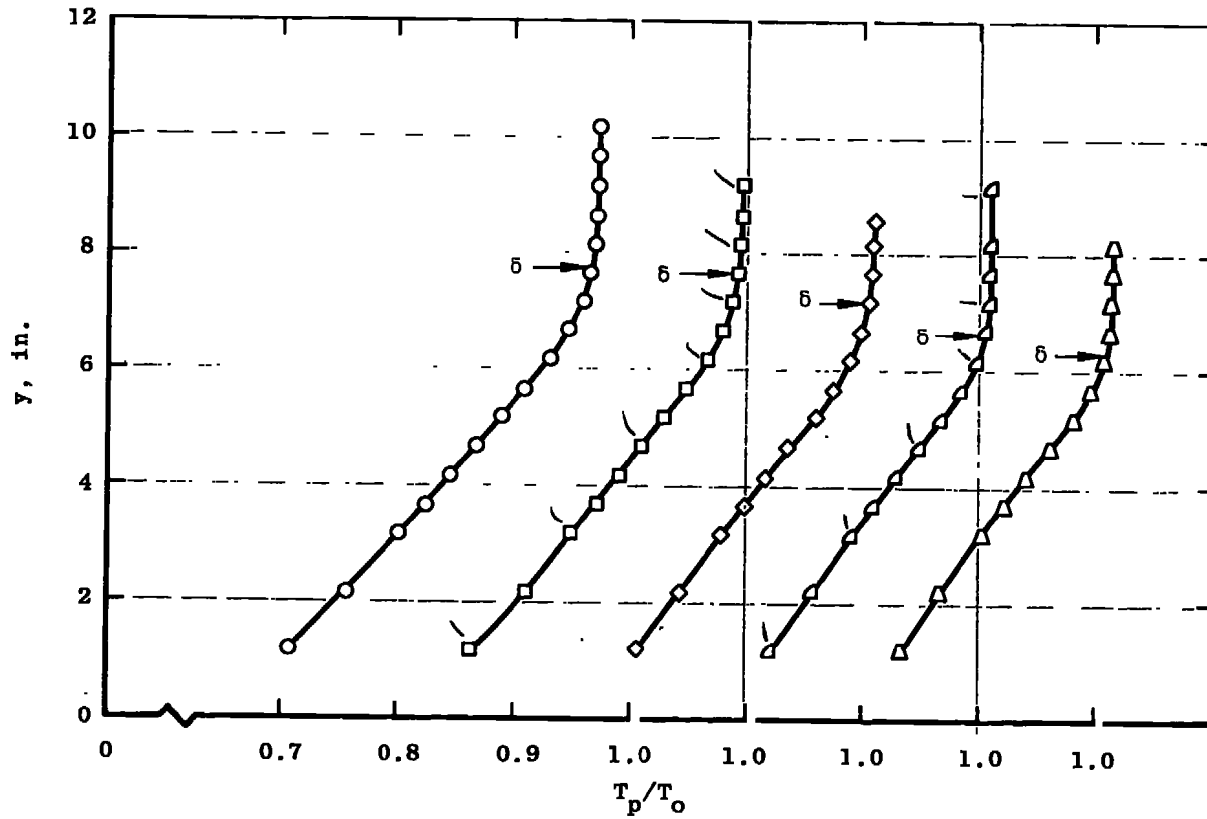
$T_w = 530^\circ R$



a. $M_e = 6$

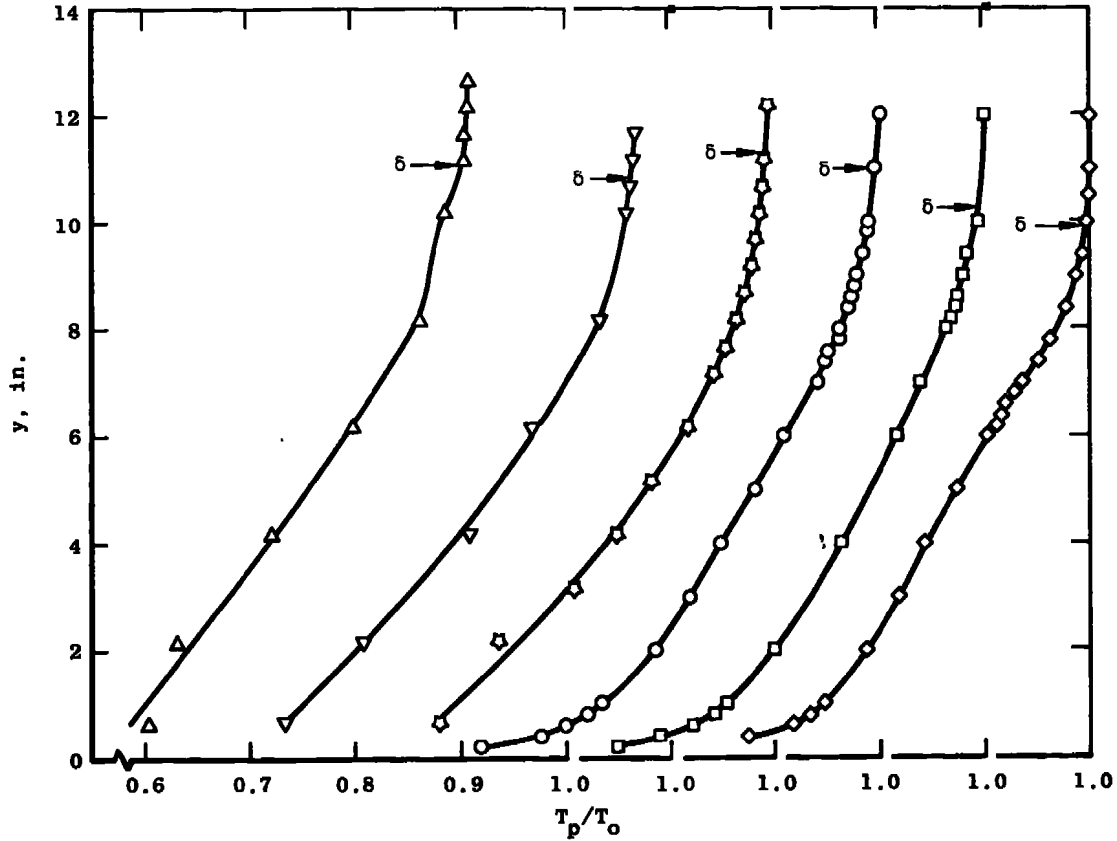
Fig. II-1 Total Temperature Profiles

Case	Sym	M_e	$Re/ft \times 10^{-6}$	$T_o, ^\circ R$	$\delta, in.$
②	○	7.90	0.44	1347	7.73
	□	7.95	0.86	1359	7.65
①	◇	7.96	1.73	1362	7.15
	△	8.02	2.69	1321	6.62
	△	8.04	3.44	1337	6.30



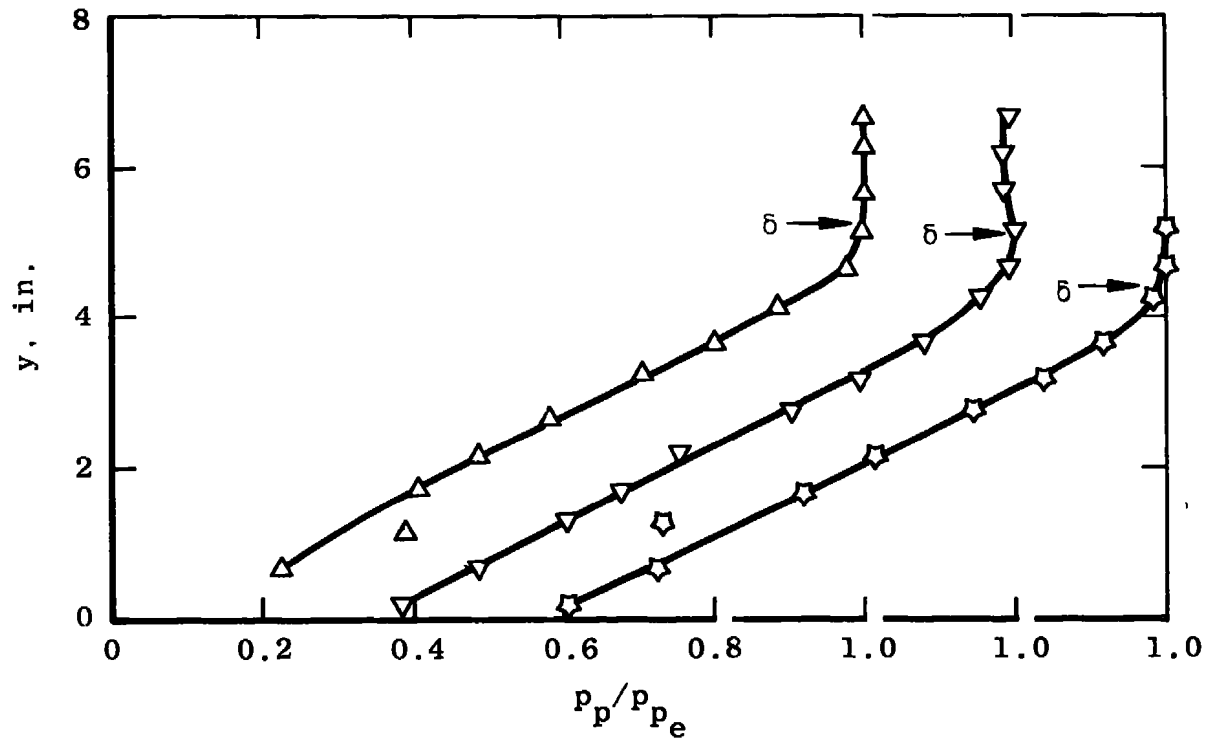
b. $M_e = 8$
Fig. II-1 Continued

Sym	M_e	$Re/ft \times 10^{-6}$	$T_o, ^\circ R$	$\delta, in.$				
Δ	9.86	0.32	1672	11.1				
∇	10.01	0.60	1714	10.8				
\star	10.06	0.83	1775	11.3				
\circ	10.10	1.14	1854	11.0				
\square	10.10	1.80	1919	\diamond	10.18	2.03	1969	9.9
\diamond	10.18	2.03	1969	9.9				



c. $M_e \approx 10$
 Fig. II-1 Concluded

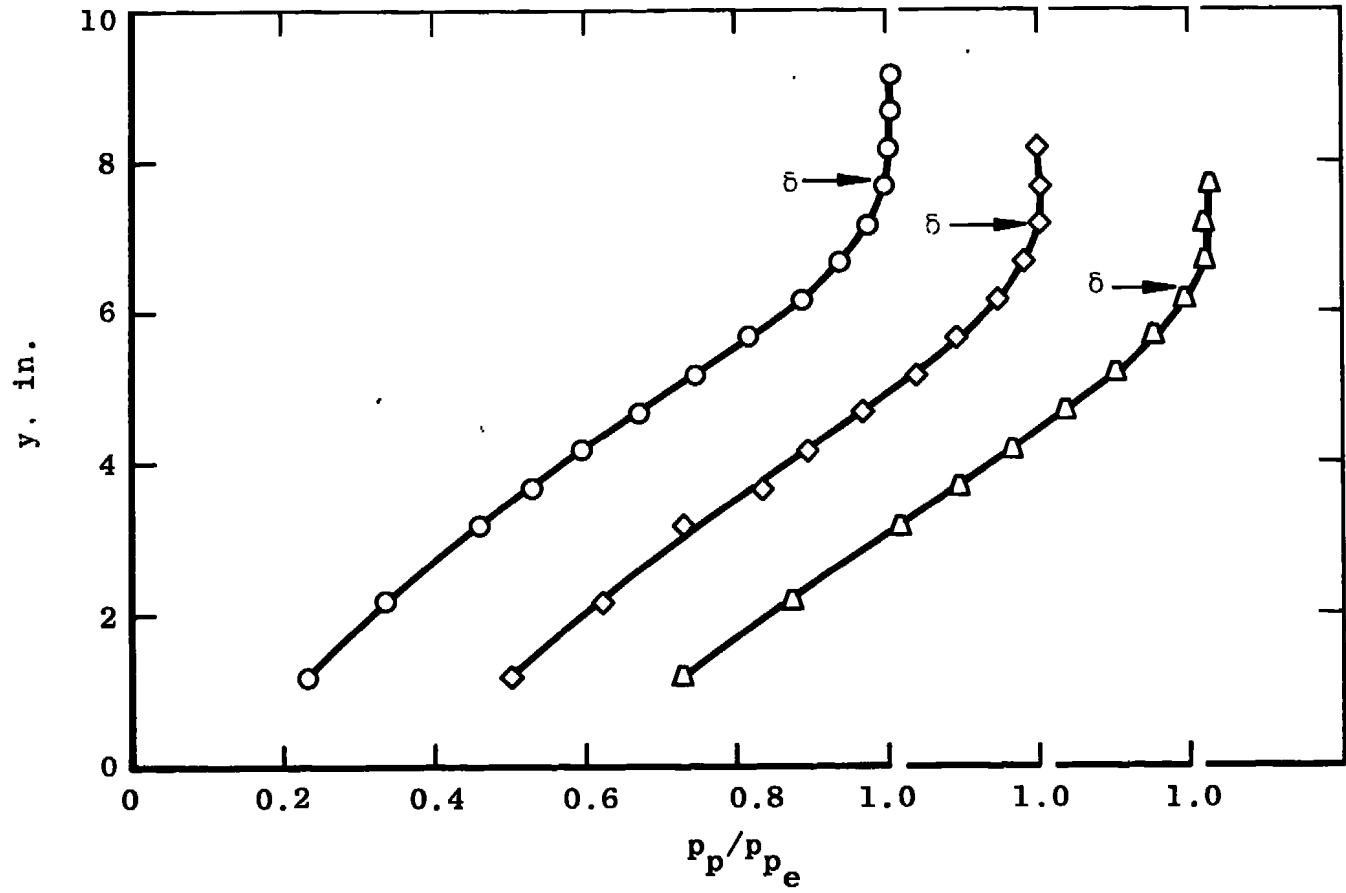
Sym	M_e	$Re/ft \times 10^{-6}$	p_{p_e} psia	δ , in. (From Fig. II-1)
Δ	5.93	1.04	1.56	5.25
∇	5.91	2.04	3.15	5.10
\star	5.95	3.91	6.15	4.40



a. $M_e = 6$

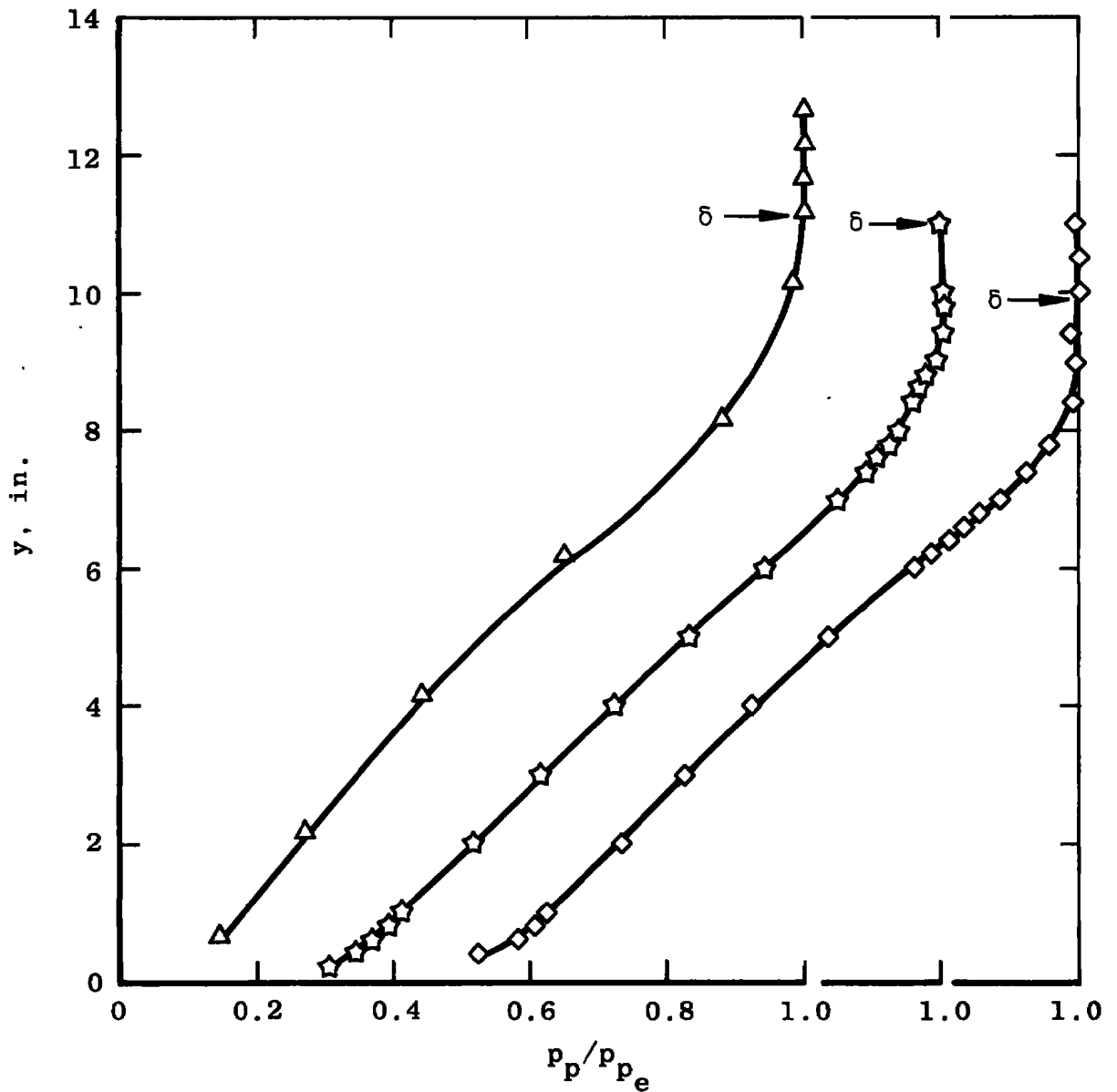
Fig. II-2 Pitot Pressure Profiles

Sym	M_e	$Re/ft \times 10^{-6}$	p_{pe} , psia	δ , in. (From Fig. II-1)
○	7.90	0.44	0.88	7.73
◇	7.96	1.73	3.47	7.15
△	8.04	3.44	6.59	6.30



b. $M_e = 8$
Fig. II-2 Continued

Sym	M_e	$Re/ft \times 10^{-6}$	p_{p_e} , psia	δ , in. (From Fig. II-1)
Δ	9.86	0.32	0.62	11.1
\star	10.10	1.14	2.53	11.0
\diamond	10.18	2.03	4.94	9.9



c. $M_e = 10$
Fig. II-2 Concluded

DOCUMENT CONTROL DATA - R & D

(Security classification of title, body of abstract and indexing annotation must be entered when the overall report is classified)

1. ORIGINATING ACTIVITY (Corporate author) Arnold Engineering Development Center ARO, Inc., Operating Contractor Arnold Air Force Station, Tennessee 37389		2a. REPORT SECURITY CLASSIFICATION UNCLASSIFIED	
		2b. GROUP N/A	
3. REPORT TITLE NOZZLE TURBULENT BOUNDARY-LAYER MEASUREMENTS IN THE VKF 50-IN. HYPERSONIC TUNNELS			
4. DESCRIPTIVE NOTES (Type of report and inclusive dates) Final Report - March to July 1965			
5. AUTHOR(S) (First name, middle initial, last name) R. K. Matthews and L. L. Trimmer, ARO, Inc.			
6. REPORT DATE June 1969		7a. TOTAL NO. OF PAGES 31	7b. NO. OF REFS 13
8a. CONTRACT OR GRANT NO. F40600-69-C-0001		9a. ORIGINATOR'S REPORT NUMBER(S) AEDC-TR-69-118	
b. PROJECT NO. G226		9b. OTHER REPORT NO(S) (Any other numbers that may be assigned this report) N/A	
c. Program 876A			
d. Program Element 65401F			
10. DISTRIBUTION STATEMENT This document is subject to special export controls and each transmittal to foreign governments or foreign nationals may be made only with prior approval of Arnold Engineering Development Center (AETS), Arnold Air Force Station, Tennessee 37389.			
11. SUPPLEMENTARY NOTES Available in DDC		12. SPONSORING MILITARY ACTIVITY Arnold Engineering Development Center (AETS), Arnold Air Force Station, Tennessee 37389	
13. ABSTRACT Pitot pressure and total temperature measurements in the tunnel wall boundary layers in the von Kármán Gas Dynamics Facility 50-in.-diam hypersonic wind tunnels are presented. The measurements were obtained in the wind tunnel test sections at nominal free-stream Mach numbers of 6, 8, and 10 at free-stream unit Reynolds numbers from 0.32×10^6 to 3.91×10^6 per foot. The boundary layers were fully turbulent (velocity profile index 6 to 10), and the total thickness ranged from 4 to 11 in. Velocity and mass flow profiles were computed and used to calculate boundary-layer displacement and momentum thicknesses. The experi- mentally determined ratio of displacement thickness to momentum thick- ness was essentially independent of Mach number and Reynolds number over the ranges investigated. This document is subject to special export controls and each transmittal to foreign governments or foreign nationals may be made only with prior approval of Arnold Engineering Development Center (AETS), Arnold Air Force Station, Tennessee 37389.			

14. KEY WORDS	LINK A		LINK B		LINK C	
	ROLE	WT	ROLE	WT	ROLE	WT
nozzle flow						
turbulent boundary layer						
wind tunnels						
pressure						
temperature						
measurement						
hypersonic flow						